Thermal comfort in indoor environment: effect of the solar radiation on the radiant temperature asymmetry

Concettina Marino, Antonino Nucara, Matilde Pietrafesa

Dipartimento di Ingegneria dell'Informazione, delle Infrastrutture e dell'Energia Sostenibile (DIIES), "Mediterranea" University of Reggio Calabria, Via Graziella - Feo di Vito, 89122, Reggio Calabria, Italy

Abstract

This paper analyzes the influence of solar radiation, considering both its direct and diffuse component, on the local thermal comfort of subjects in indoor environments. More precisely, an original equation for the assessment of the plane radiant temperature in presence of solar radiation is proposed. It can be used to evaluate the correspondent radiant asymmetry and therefore allows detailed analysis of local thermal discomfort conditions. Its reliability and feasibility have been tried out by means of an application to a simple case study and the obtained results proved that, in the studied environment, solar radiation affects the symmetry of the radiant field to a considerable extent, being the main cause of local discomfort due to not acceptable values of the radiant asymmetry. Therefore, the method can be used to verify the presence of zones not suited to human activities inside rooms and, in addition, it can be exploited by the procedures aimed at the classification of the comfort quality of indoor environments.

Keywords

Solar Radiation; Thermal Comfort; Local thermal discomfort; Radiant temperature asymmetry.

1 Introduction

Nowadays, the increasing level of life quality towards the highest standards requires the extremely precise definition of the microclimatic conditions suited to ensuring people's thermal comfort in spaces where human activities are performed. Moreover, comfort and energy demand in buildings are strongly

interrelated and the achievement of high quality standards involves an energy cost which must be taken into account (Calvino et al., 2010; Marino et al., 2015a).

The human thermal comfort sensation is strictly related to the metabolic heat production, to the energy exchanges between the human body and the environment and to the consequent variations of the physiological parameters (Fanger, 1970).

A too hot or too cold sensation may regard the human body as a whole, so that the subject experiences a generalized discomfort sensation: this case is called “global thermal discomfort” which is generally assessed by means of the Fanger’s PMV and PPD-indexes, described in the ISO 7730 (ISO, 2005) and based on the 7-point ASHRAE thermal sensation scale (ASHRAE, 2010).

In order to asses global comfort conditions, average values of the microclimatic parameters are generally used; nevertheless, in many practical cases, this approach does not allow a correct appraisal of the environmental quality of the indoor space on the grounds that the space and time variability of the physical parameters should be taken into account (Marino et al., 2015b; Simone et al., 2013).

In addition, a sensation of thermal discomfort can be also caused by an undesired local cooling or heating of a particular area of the body: this case is called "local thermal discomfort".

The main causes of local discomfort are: significant vertical air temperature differences, atypical floor temperatures, air drafts and significant radiant asymmetry (Fanger, 1970; Rizzo et al., 2004).

Among these issues, the radiant asymmetry, which is the difference between the plane radiant temperatures of two opposite faces of a plane element called "test area", is a parameter measuring the uniformity of the radiant field surrounding the subject. Indeed, the presence of too hot or too cold surfaces may alter this uniformity, so that different parts of the body, not uniformly exposed, might reach different temperatures which, in turn, may be cause of discomfort sensations for the subject.

Experimental studies conducted on a large number of people have shown that the number of dissatisfied subjects grows rapidly as the radiant asymmetry rises (Fanger et al., 1985, 1980). This effect is even more enhanced by solar radiation, which can make the radiant field dramatically asymmetric.

As a matter of fact, solar radiation entering the indoor space through the windows not only strongly affects the global thermal balance of the human body directly hit by the ray, but also causes a local heating of a particular area of the body and, therefore, raises the radiant asymmetry.

In order to take into account this phenomenon, the aim of this article is to propose an original equation for the assessment of the plane radiant temperature in presence of solar radiation. It can be used to evaluate the correspondent radiant asymmetry and therefore allows detailed analysis of local thermal discomfort conditions.

2 Plane radiant temperature

The plane radiant temperature is defined as the uniform temperature of an enclosure where the radiative flux on one side of a small plane element, the so called "test area", is the same as in the actual environment (ISO, 2001).

In order to infer an analytical relation for the plane radiant temperature, the radiative heat fluxes regarding the test area (Fig. 1) must be analyzed.

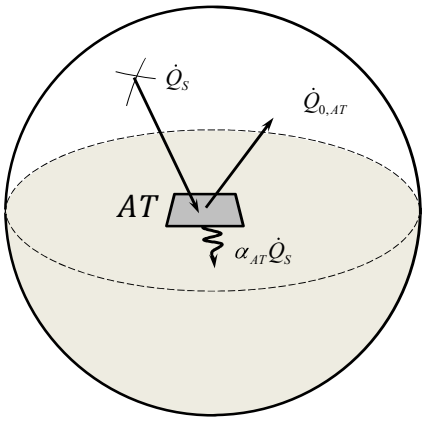

Fig. 1 - Radiative heat fluxes regarding the test area.

Inside an enclosed concave environment, the radiative net flow $\dot{Q}_{AT}$ leaving the surface named "test area" is equal to the thermal flux, $\dot{Q}_{AT\leftrightarrow S}$, exchanged between the test area and the environment (La Gennusa et al., 2005), that is:

$$\dot{Q}_{AT\leftrightarrow S} = \dot{Q}_{AT} \tag{1}$$

In turn, the net flow leaving the surface is equal to the difference between the emitted and the absorbed flux:

$$\dot{Q}_{AT} = \dot{Q}_{0,AT} - \alpha_{AT}\dot{Q}_S \tag{2}$$

in which $\dot{Q}_{0,AT}$ is the emitted flux, $\dot{Q}_S$ the thermal flow coming from the environment and α_{AT} the absorption coefficient of the test area.

2.1 Emitted thermal flow

Assuming that T_{AT} is the absolute temperature of the test area, the corresponding emitted thermal flow is:

$$\dot{Q}_{0,AT} = \sigma\varepsilon_{AT}A_{AT}T_{AT}^4 \tag{3}$$

where σ is the Stefan–Boltzmann constant, ε_{AT}, A_{AT} and T_{AT} are the emissivity, the surface and the absolute temperature of the test area, respectively.

2.2 Thermal flow coming from the environment

The thermal flow that reaches the test area is the sum of the long wave radiation coming from the surfaces of the environment, $\dot{Q}_{env\to AT}$, and the short wave solar radiation passing through the windows, $\dot{Q}_{sun\to AT}$:

$$\dot{Q}_S = \dot{Q}_{env\to AT} + \dot{Q}_{sun\to AT} \tag{4}$$

2.2.1 Radiant flow from the walls of the environment

With reference to Fig. 2, assuming that the *N* walls of the environment can be considered as black bodies, the total radiant flow coming from the environment and reaching the test area may be expressed by the following equation:

$$\dot{Q}_{env\to AT} = \sum_{i=1}^{N}\dot{Q}_{i\to AT} = \sigma\sum_{i=1}^{N}F_{i\to AT}A_iT_i^4 \tag{5}$$

where A_i and T_i are the area and the temperature of the ith isothermal surface of the environment respectively, whereas $F_{i\to AT}$ is the view factor between the ith isothermal surface and the test area.

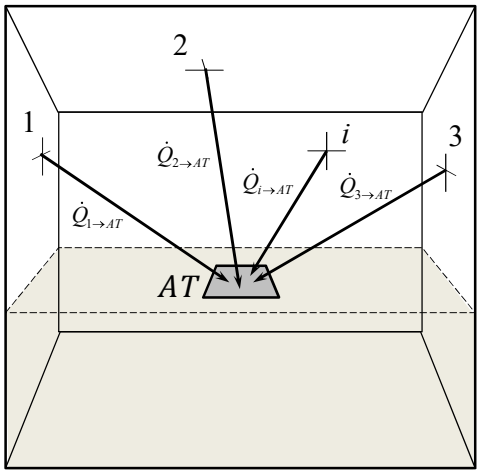

Fig. 2 - Radiative exchanges between a confined environment and the test area.

Considering the reciprocity rule of view factors, which is:

$$F_{i\to AT} A_i = F_{AT\to i} A_{AT} \tag{6}$$

Eq. (5) can be written as:

$$\dot{Q}_{env\to AT} = \sigma A_{AT} \sum_{i=1}^{N} F_{AT\to i} T_i^4 \tag{7}$$

Whereas view factors among environment and human body depend on the shape of the subject and need appropriate approaches to be evaluated (Calvino et al., 2005; La Gennusa et al., 2008; Rizzo et al., 1992; Tanabe et al., 2000), on the contrary, view factors between the test area and the surfaces of the environment may be calculated by means of the typical geometrical approach which leads to a fairly simple analytical formula.

As a matter of fact, with reference to Fig. 3, view factors between the test area and the rectangular surfaces of the environment can be evaluated using the following relationships (ISO 1998):

Case a) Parallel surfaces

$$F_{AT\to i} = \frac{1}{2\pi}\left[\frac{a/c}{\sqrt{1+(a/c)^2}}\tan^{-1}\frac{b/c}{\sqrt{1+(a/c)^2}} + \frac{b/c}{\sqrt{1+(b/c)^2}}\tan^{-1}\frac{a/c}{\sqrt{1+(b/c)^2}}\right] \tag{8}$$

Case b) Orthogonal surfaces

$$F_{AT\to i} = \frac{1}{2\pi}\left[\tan^{-1}\frac{1}{(c/b)} - \frac{c/b}{\sqrt{(a/b)^2+(c/b)^2}}\tan^{-1}\frac{1}{\sqrt{(a/b)^2+(c/b)^2}}\right] \tag{9}$$

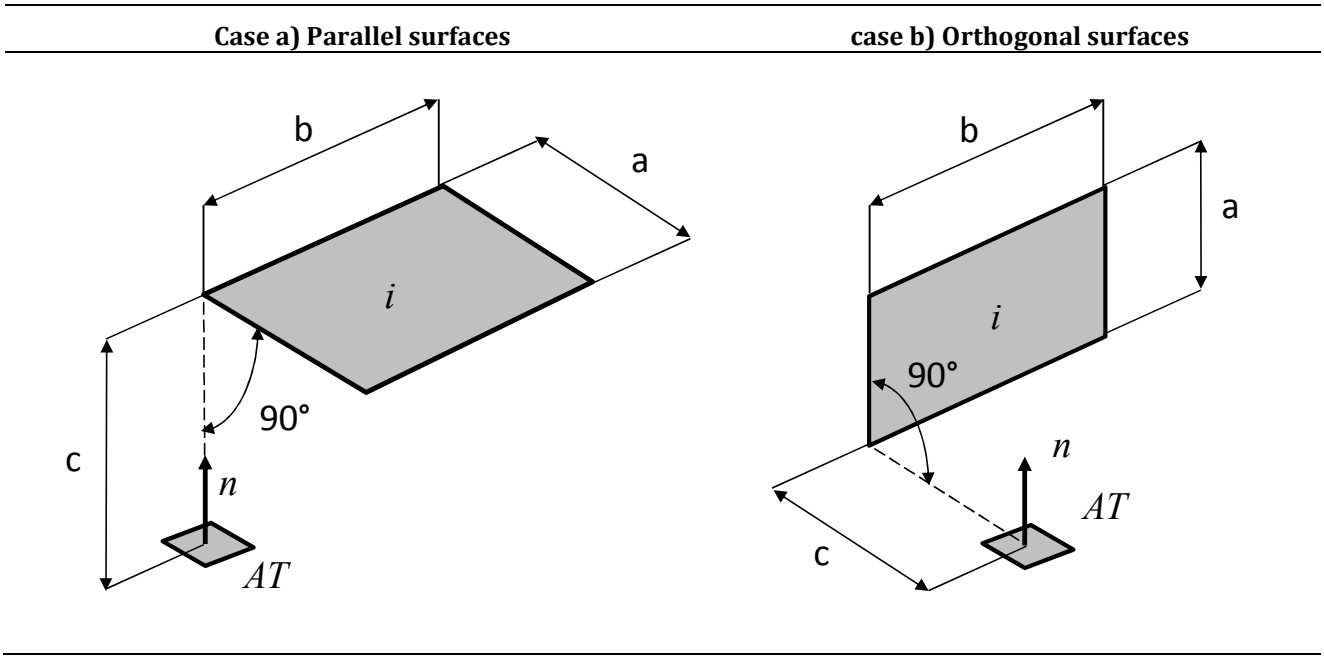

Fig. 3 – Geometric configurations suitable for the calculation of the angle factor.

2.2.2 Heat flow from the sun

The contribution of solar radiation, $\dot{Q}_{sun \to AT}$, consists of two components related to diffuse radiation, $\dot{Q}_{d \to AT}$, and to direct radiation, $\dot{Q}_{b \to AT}$, respectively:

$$\dot{Q}_{sun \to AT} = \dot{Q}_{d \to AT} + \dot{Q}_{b \to AT} \tag{10}$$

In the hypothesis that the diffuse radiation entering the environment through glazed surfaces follows the Lambert's law, its contribution to the radiative flux on the test area is given by:

$$\dot{Q}_{d \to AT} = \sum_{j=1}^{M} F_{j \to AT} A_j I_d \tag{11}$$

being $F_{j \to AT}$ the view factor between the jth glazed surface and the test area, A_j the area of the jth glazed surface, and I_d the intensity of the diffuse solar radiation on the test area.

Hence, exploiting the reciprocity rule, the eq. (11) can be expressed as:

$$\dot{Q}_{d \to AT} = I_d A_{AT} \sum_{j=1}^{M} F_{AT \to j} \tag{12}$$

with the view factor $F_{AT \to j}$ calculated with the equations (8) e (9).

On the other side, the contribution due to the direct radiation can be calculated by means of:

$$\dot{Q}_{b\to AT} = A_{AT} I_{b\perp} \tag{13}$$

where $I_{b\perp}$ is the component of the beam solar radiation perpendicular to the surface of the test area.

Using the relationships (3), (7), (12) and (13) in Eq. (2), the net heat flow from the test area, located in the real non-uniform thermal environment of Fig. 2, can be obtained:

$$\dot{Q}_{AT} = \sigma\varepsilon_{AT} A_{AT} T_{AT}^4 - \alpha_{AT}\left(\sigma A_{AT}\sum_{i=1}^{N} F_{AT\to i} T_i^4 + I_d A_{AT}\sum_{j=1}^{M} F_{AT\to j} + A_{AT} I_{b\perp}\right) \tag{14}$$

Therefore, using equation (14), the flow exchanged between the test area and the environment can be inferred from equation (1):

$$\dot{Q}_{AT\leftrightarrow S} = \sigma\varepsilon_{AT} A_{AT} T_{AT}^4 - \alpha_{AT}\left(\sigma A_{AT}\sum_{i=1}^{N} F_{AT\to i} T_i^4 + I_d A_{AT}\sum_{j=1}^{M} F_{AT\to j} + A_{AT} I_{b\perp}\right) \tag{15}$$

Indeed, on the basis of the previously reported definition of plane radiant temperature, in the hypothesis that the test area may be considered as a small surface with respect to the environment dimensions (Fig. 4), the thermal heat flow $\dot{Q}_{AT\leftrightarrow S}$ can also be calculated as follows:

$$\dot{Q}_{AT\leftrightarrow S} = \sigma\varepsilon_{AT} A_{AT}\left(T_{AT}^4 - T_{pr}^4\right) \tag{16}$$

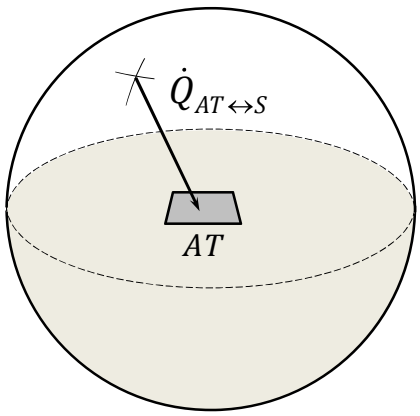

Fig. 4 - Radiative exchanges between a black enclosure and the test area.

Therefore, considering equations (15) and (16), the following equation can be written:

$$\sigma\varepsilon_{AT} A_{AT} T_{AT}^4 - \alpha_{AT}\left(\sigma A_{AT}\sum_{i=1}^{N} F_{AT\to i} T_i^4 + I_d A_{AT}\sum_{j=1}^{M} F_{AT\to j} + A_{AT} I_{b\perp}\right) = \sigma\varepsilon_{AT} A_{AT}\left(T_{AT}^4 - T_{pr}^4\right) \tag{17}$$

which yields:

$$T_{pr} = \sqrt[4]{\frac{\alpha_{AT}}{\varepsilon_{AT}} \sum_{i=1}^{N} F_{AT \to i} T_i^4 + \frac{\alpha_d}{\sigma \varepsilon_{AT}} I_d \sum_{j=1}^{M} F_{AT \to j} + \frac{\alpha_b}{\sigma \varepsilon_{AT}} I_{b\perp}} \tag{18}$$

The three absorption coefficients α_{AT} , α_d and α_b, are referred to infrared radiation, diffuse solar radiation and direct solar radiation respectively.

By and large, they are supposed to assume different values depending on both the radiation's wavelength and the temperature of the source (Fig. 5). Therefore, whereas the area test may be assumed to behave as a blackbody (with $\alpha_{AT} = 1$) when infrared radiation is taken into account, on the contrary, this hypothesis is not reliable when the solar radiation is considered. In this case, indeed, being about 5780 K the surface temperature of the sun, the absorption coefficients for diffuse and direct solar radiation can be assumed equal to 0.7 (Fig. 5).

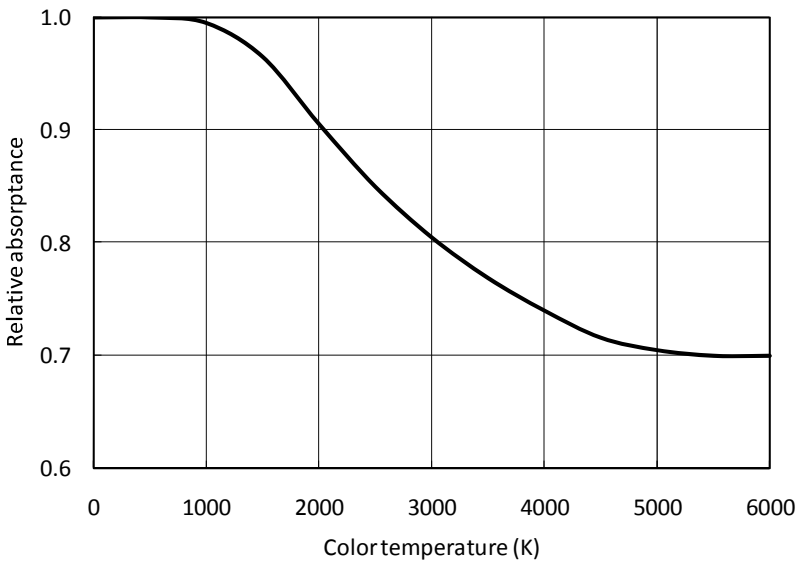

Fig. 5 – Absorbance coefficient versus the temperature of the emitting source (ASHRAE, 1989).

The expression (18) is then simplified as follows:

$$T_{pr} = \sqrt[4]{\sum_{i=1}^{N} F_{AT \to i} T_i^4 + \frac{0.7}{\sigma} \left(I_d \sum_{j=1}^{M} F_{AT \to j} + I_{b\perp} \right)} \tag{19}$$

3 Radiant temperature asymmetry

The radiant temperature asymmetry is the difference between the plane radiant temperature of the two opposite sides of a small plane element (ISO, 1998).

For assessments of local discomfort, the radiant temperature asymmetry is evaluated with reference to three orthogonal directions. Therefore, the calculation of six plane radiant temperatures (Fig. 6) allows the asymmetry in the directions X, Y and Z to be assessed. As a consequence, three plane elements respectively orthogonal to the axis X, Y, Z must be considered and, hence, six test areas (one on each side of each plane element) must be taken into account.

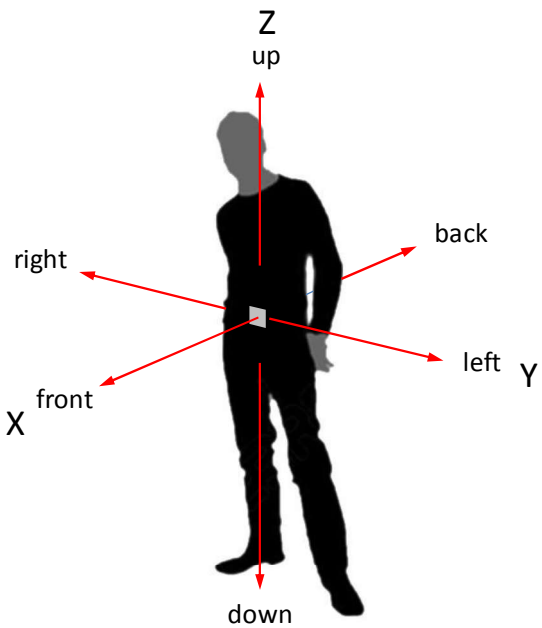

Fig. 6 - Reference system feasible for the calculation of the radiant asymmetry.

In order to calculate the plane radiant temperature for each of the six test areas considering the effect of the solar radiation, the direct radiation striking each test area, $I_{b\perp}$, must be reckoned .

This component can be calculated provided that the angle of incidence θ, which is the angle between the line normal to the surface and the solar rays (Fig. 7), is known.

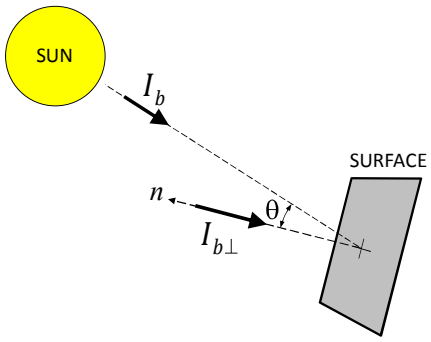

Fig. 7 – Angle of incidence.

It depends on a set of angles characterizing the position of the sun and the inclination and orientation of the surface, namely: the solar altitude α, the solar azimuth γ, the tilt angle β between the surface and the horizontal plane, the surface azimuth ξ, equal to the angle between the projection of the normal to the surface on a horizontal plane and the South; in fact it can be assessed as:

$$\cos\theta = \cos\alpha\cos(\gamma-\xi)\sin\beta + \sin\alpha\cos\beta \tag{20}$$

This relationship needs to be particularized for each of the six test areas which is required for assessing the radiant asymmetry. To reach this goal, for every test area, the tilt angle β, and the surface azimuth, ξ, must be evaluated.

Assuming that ξ_0 is the angle between the positive direction of the X axis (Fig. 6) and the South, the values of both the tilt angle β and the surface azimuth, ξ, and the consequent expressions of the incidence angle, θ, are reported in Tab. 1, for each test area, which, in turn, is identified by means of the direction of its normal line (namely the axis X, Y or Z) and of the sign (+) or (-) referred to its orientation (namely front, back, etc.).

Tab. 1 – Relationships expressing the incidence angle between the solar rays and the line normal to the test area.

Direction	β	ξ	θ
front (X^+)	90°	ξ_0 +0°	$\cos^{-1}[\cos\alpha\cos(\gamma-\xi)]$
back (X^-)		ξ_0 +180°	
left (Y^+)		ξ_0 +270°	
right (Y^-)		ξ_0 +90°	
up (Z^+)	0°	Any	$\cos^{-1}(\sin\alpha)$

down (Z^-)	180°	Any	$\cos^{-1}(-\sin\alpha)$

Knowing the incidence angle θ, the direct radiation on the test area can be assessed:

$$I_{b\perp} = I_b \cos\theta \tag{21}$$

being I_b the intensity of the direct normal radiation.

Thus, the equation (19) can be modified as follows:

$$T_{pr} = \sqrt[4]{\sum_{i=1}^{N} F_{AT\to i} T_i^4 + \frac{0.7}{\sigma}\left(I_d \sum_{j=1}^{M} F_{AT\to j} + I_b \cos\theta \right)} \tag{22}$$

The second term of equation (22) represents the effect of the sun and hence must be set to zero during the night.

Furthermore, in real environments, obstructions, like building walls or shading devices, can shade the direct component of the solar radiation on the test area; in this case the third term of equation (22) must be set to zero.

In addition, the test area may not be facing the sun, being in its own shadow, in this case the third term of equation (22) must be set to zero, as well.

With a view to considering the effect of these phenomena, three coefficients have been introduced in equation (22):

1) the *day–night coefficient*, C_{dn}, equal to 1 during daytime and equal to 0 during the nighttime;
2) the *obstruction coefficient*, C_o, equal to 1 when the test area is directly hit by the solar beam and equal to 0 in the other cases;
3) the *own-shadow coefficient*, C_s, equal to 1 when the test area is in its own shadow and equal to 0 in the other cases.

Under these hypotheses, the equation (22) becomes:

$$T_{pr} = \sqrt[4]{\sum_{i=1}^{N} F_{AT\to i} T_i^4 + \frac{0.8 \times C_{dn}}{\sigma}\left(I_d \sum_{j=1}^{M} F_{AT\to j} + C_o C_s I_b \cos\theta \right)} \tag{23}$$

As regards the coefficients in Eq. (23), the parameter C_{dn} can be evaluated with reference to the sunrise time, h_{sr}, and sunset time, h_{ss}:

$$\begin{cases} h_{sr} = 12 - \dfrac{\cos^{-1}(-\tan\varphi\tan\delta) - 180}{15} \\ h_{ss} = 12 + \dfrac{\cos^{-1}(-\tan\varphi\tan\delta) - 180}{15} \end{cases} \tag{24}$$

where φ is the site latitude and δ is the declination angle.

The value of the coefficient C_{dn} at the solar time h is:

$$\begin{cases} C_{dn} = 1 & \textit{if} \quad h_{sr} < h < h_{ss} \\ C_{dn} = 0 & \textit{otherwise} \end{cases} \tag{25}$$

On the other hand, the parameter C_o can be evaluated with reference to the angles depicted in Fig. 8. It is:

$$\begin{cases} C_o = 1 & \textit{if} \quad \alpha_{01} < \alpha < \alpha_{02} \quad \textit{and} \quad \gamma_{01} < \gamma < \gamma_{02} \\ C_o = 0 & \textit{otherwise} \end{cases} \tag{26}$$

In addition, as regards the own-shadow coefficient, C_s, it can be assessed as follows:

$$\begin{cases} C_s = 1 & \textit{if} \quad \cos\theta > 0 \\ C_s = 0 & \textit{otherwise} \end{cases} \tag{27}$$

Finally, calculated the plane radiant temperature, the radiant asymmetry may be assessed, for each direction (Fig. 6), as follows:

$$\Delta t_{pr} = \Delta T_{pr} = \sqrt[4]{T_{pr(+)}^4} - \sqrt[4]{T_{pr(-)}^4} \tag{28}$$

where the signs (+) and (-) respectively refer to each face (namely a test area) of each plane correspondingly normal to the considered directions X, Y and Z (Tab. 1).

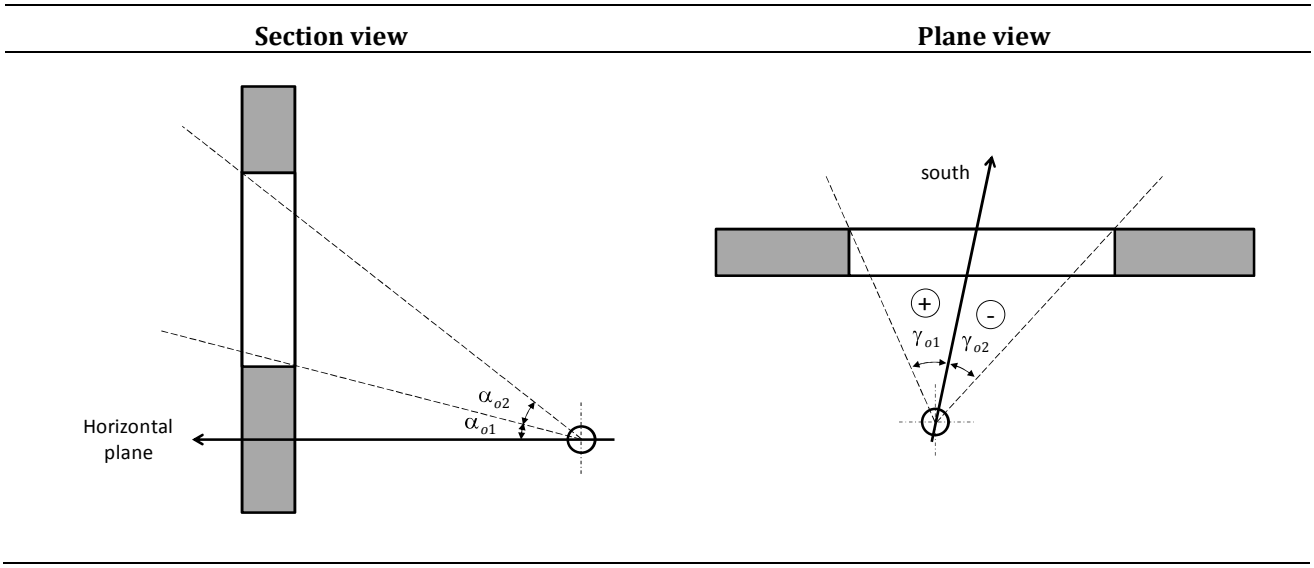

Fig. 8 – Angles needed for the evaluation of the obstruction coefficient.

4 An application

In the present section, the proposed model will be clarified through an example.

4.1 Building module

Considering the plain building module depicted in Fig. 9, an analysis of the spatial and temporal variations of the radiant field has been carried out at the height of 0.80 m above the floor. More precisely, radiant asymmetry was assessed at the points shown in Fig. 9. The module is located in Reggio Calabria (38°7'15" North, 15°39'53" East), a Southern Italian town characterized by a Mediterranean mild climate. The analysis has been carried out in winter, on December 21st, and has involved a period of 24 hours.

For each considered point, the X-axis of the reference system, reported in Fig. 6, is lined up with the North-South direction and points South (ξ_0 =0°), the Y axis is parallel to the East-West direction and points East, the Z axis is normal to the XY plane and points upward.

As regards the orientation of the test areas, the following conventions were utilized:

– the South facing area and the North facing one, both normal to the X direction, were singled out with the symbols X^+ and X^- respectively;

- the East facing area and the West facing one, both normal to the Y direction, were identified by the symbols Y^+ and Y^- respectively;
- the upward facing area and the downward facing one, both normal to the Z direction, were identified by the symbols Z^+ and Z^- respectively.

The temperature of all the internal surfaces of the building module has been assumed equal to 20°C, while the optical transmittance of the glazed surface at normal incidence of the rays has been assumed equal to 0.87. The view factors between the test area and the glazed surface, calculated with the eq. (8) and (9), are reported in Tab. 2.

The equations (23) and (28) have been utilized with a view to evaluating the plane radiant asymmetry along the X, Y and Z directions and an index, the *EQI* (Marino et al., 2015b, 2012), has been assessed in order to classify the comfort quality of the indoor environment with reference to the radiant field.

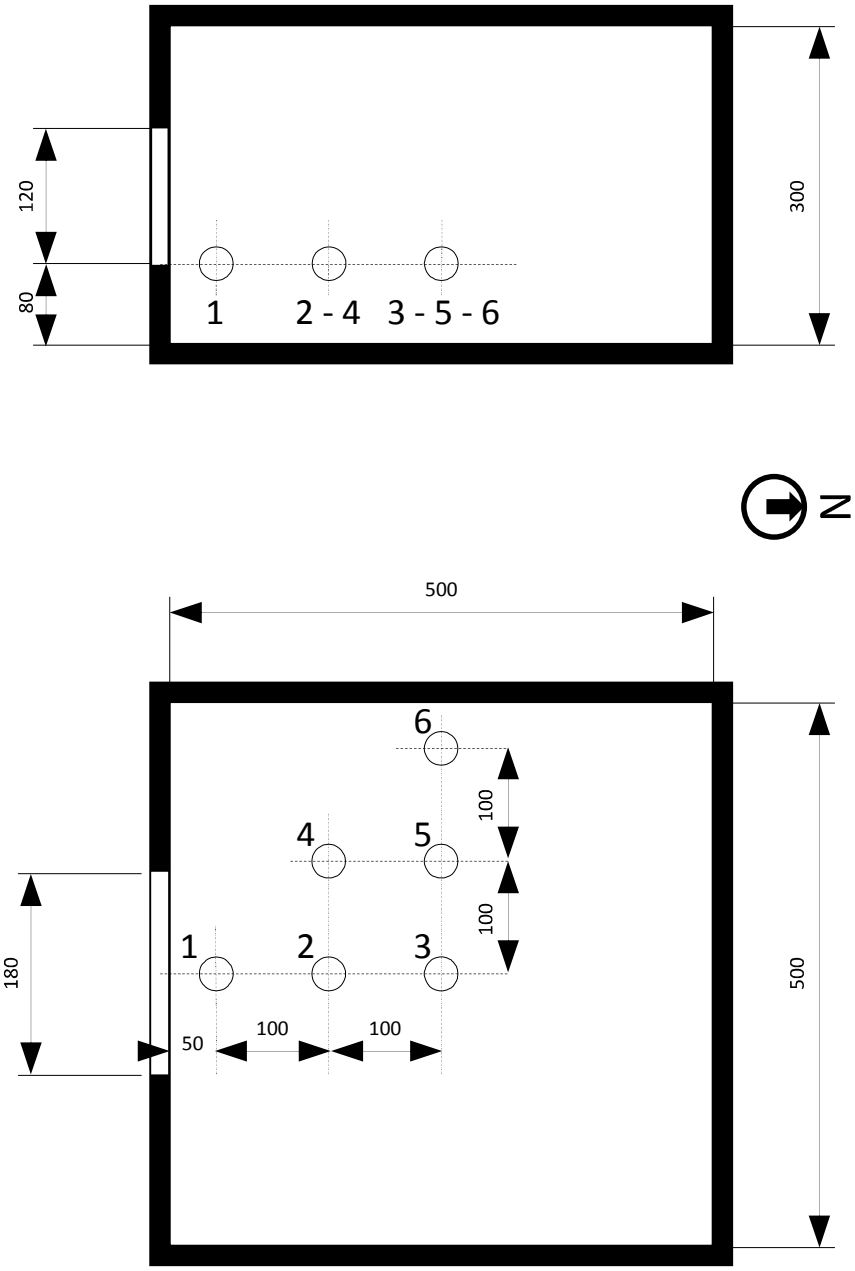

Fig. 9 – Building module.

Tab. 2 - View factors between the test area and the glazed surface for each considered point.

Point	X^+	X^-	Y^+	Y^-	Z^+	Z^-
1	0.418	0.000	0.264	0.264	0.132	0.000
2	0.186	0.000	0.063	0.063	0.032	0.000
3	0.089	0.000	0.020	0.020	0.010	0.000
4	0.123	0.000	0.047	0.000	0.043	0.000
5	0.071	0.000	0.016	0.000	0.016	0.000
6	0.040	0.000	0.009	0.000	0.009	0.000

4.2 Calculation of the solar radiation

The first step of the procedure has regarded the assessment of the solar path and of the obstruction angles of the window depicted in Fig. 8; knowing these factors the shadow periods due to the building shape (Fig. 10) and, consequently, the obstruction coefficients can be evaluated for each considered point.

Successively, the hourly direct and diffuse components of the solar radiation shining on a horizontal surface (respectively I_{dh} and I_{bh}) have been evaluated by means of the Liu and Jordan method (Liu and Jordan, 1960), knowing the monthly average daily global solar radiation on the horizontal surface, which, for the considered site, is equal to 6.9 MJ/m^{2}day (Huld et al., 2012). The calculated two components of solar radiation are reported in Fig. 11.

The following stage of the procedure, hence, has regarded the calculation of the solar radiation entering the indoor environment through the glazed surface. To pursue this goal, a series of hypothesis were made: a) the beam component maintains its direction crossing the glass; b) the diffuse component is considered to cross the glass layer as a direct radiation having an intensity equal to the diffuse one, an altitude angle of 60°, and an azimuth angle, evaluated with respect to the normal to the surface, equal to 0; c) the diffuse radiation entering the room through the glazed surfaces follows the Lambert's law.

In this case, the direct normal radiation and the diffuse component complying with the hypothesis b), both shining on the external side of the glazed surface, can be assessed by means of the following equations (La Gennusa et al., 2007):

$$\begin{cases} I_b^{out} = \dfrac{I_{bh}}{\sin\alpha} \\ I_d^{out} = \dfrac{\rho}{4}\left(I_{bh} + I_{dh}\right) + \dfrac{3}{4} I_{dh} \end{cases} \tag{29}$$

where α is the solar altitude and ρ is the albedo, assumed equal to 0.3.

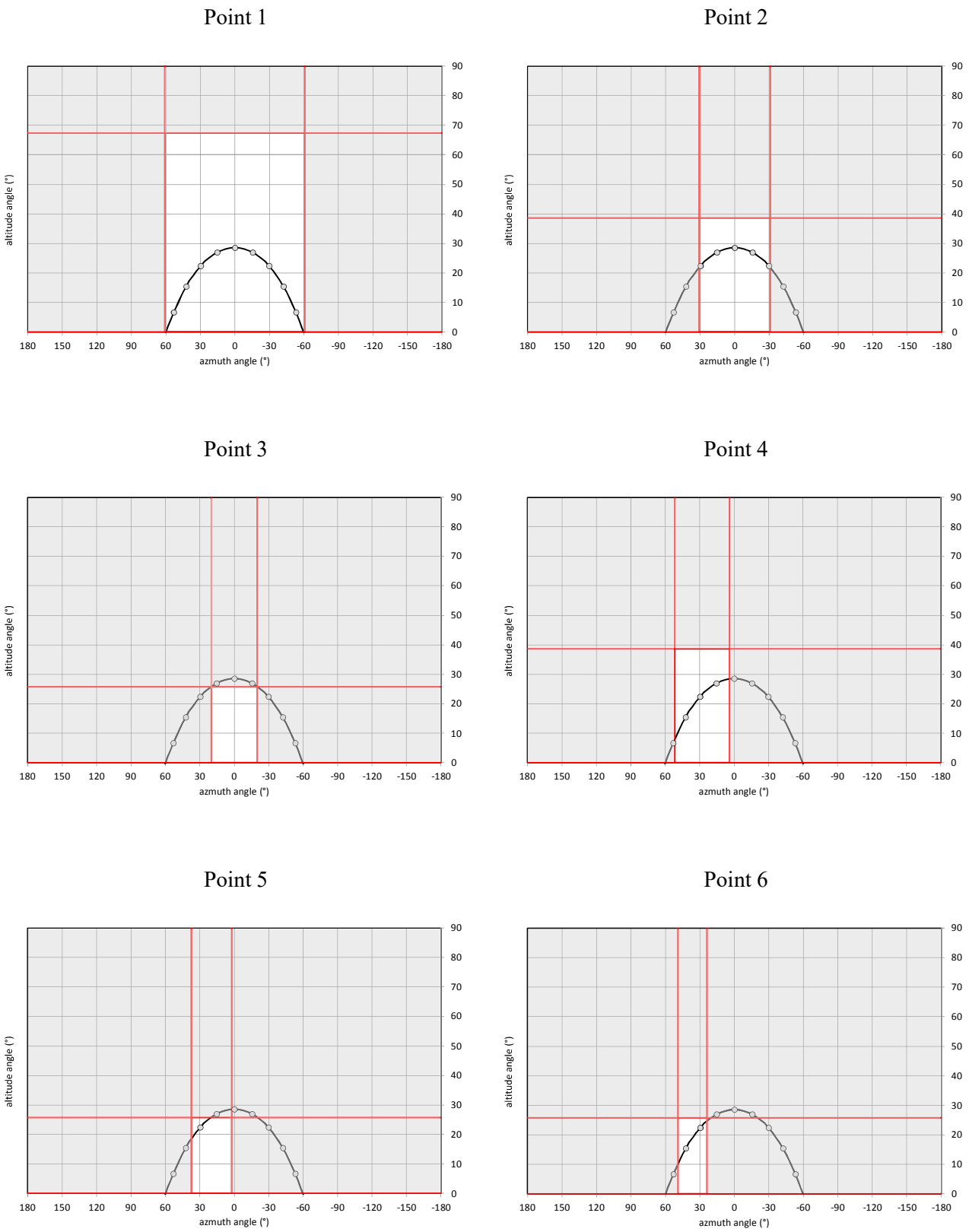

Fig. 10 – Shadow periods due to the building shape, at each examined point .

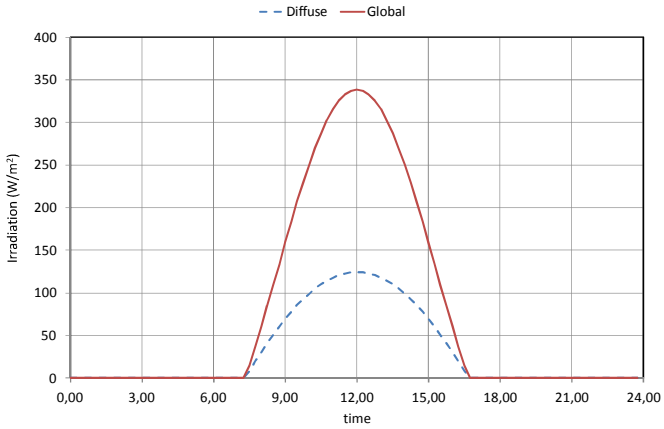

Fig. 11 - Hourly solar radiation on a horizontal surface in outdoor environments.

Therefore, the intensity of solar radiation entering the indoor environment can be evaluated as:

$$\begin{cases} I_b^{in} = \tau_b I_b^{out} \\ I_d^{in} = \tau_d I_d^{out} \end{cases} \tag{30}$$

where τ_b and τ_d are the optical transmittances of the glass for the direct and diffuse component respectively. They may be calculated using the SHGF procedure proposed by ASHRAE (ASHRAE, 1989), which express the optical transmittances as:

$$\tau_b = \frac{\sum_{j=0}^{5} \tau_j \cos^j \Theta}{0.86} \tau_n \tag{31}$$

in which Θ is the angle between the solar rays and the line normal to the glass surface and τ_n is the optical transmittance of the glazed surface at normal incidence of the solar rays. The values assumed by the τ_j coefficients are reported in Tab. 3.

Tab. 3 – Coefficients for the calculation of the optical transmittance of the glass with the SHGF procedure (ASHRAE, 1989).

j	τ_j
0	-0.0089
1	2.71235
2	-0.6206
3	-7.0733
4	9.75995
5	-3.8992

The values of the solar radiation components calculated by means of Eqs. (29) and (30) are reported in Fig. 12 where, as far as the indoor direct normal radiation (I_b^{in}) is concerned, the calculated shadow periods, characterizing each examined point, are taken into account.

At this stage of the procedure, by means of eq. (21) combined with the equations reported in Tab. 1, the direct radiation hitting the test areas is able to be assessed. The results of this calculation are reported in Fig. 13, where the interaction with the shadow patterns owing to the window geometry is also depicted.

By and large, it is worth noting that:

a) along the X direction, solar radiation usually comes from South and hits the X^+ test area, but there is no contribution from North on the X^- test area;
b) along the Y direction, before 12 a.m., solar radiation comes from East, hitting the Y^+ test area; afterward it comes from West and hence affects the Y^- test area;
c) along the Z direction, the radiation always comes from above and therefore only the Z+ test area is involved for the whole daylight period.

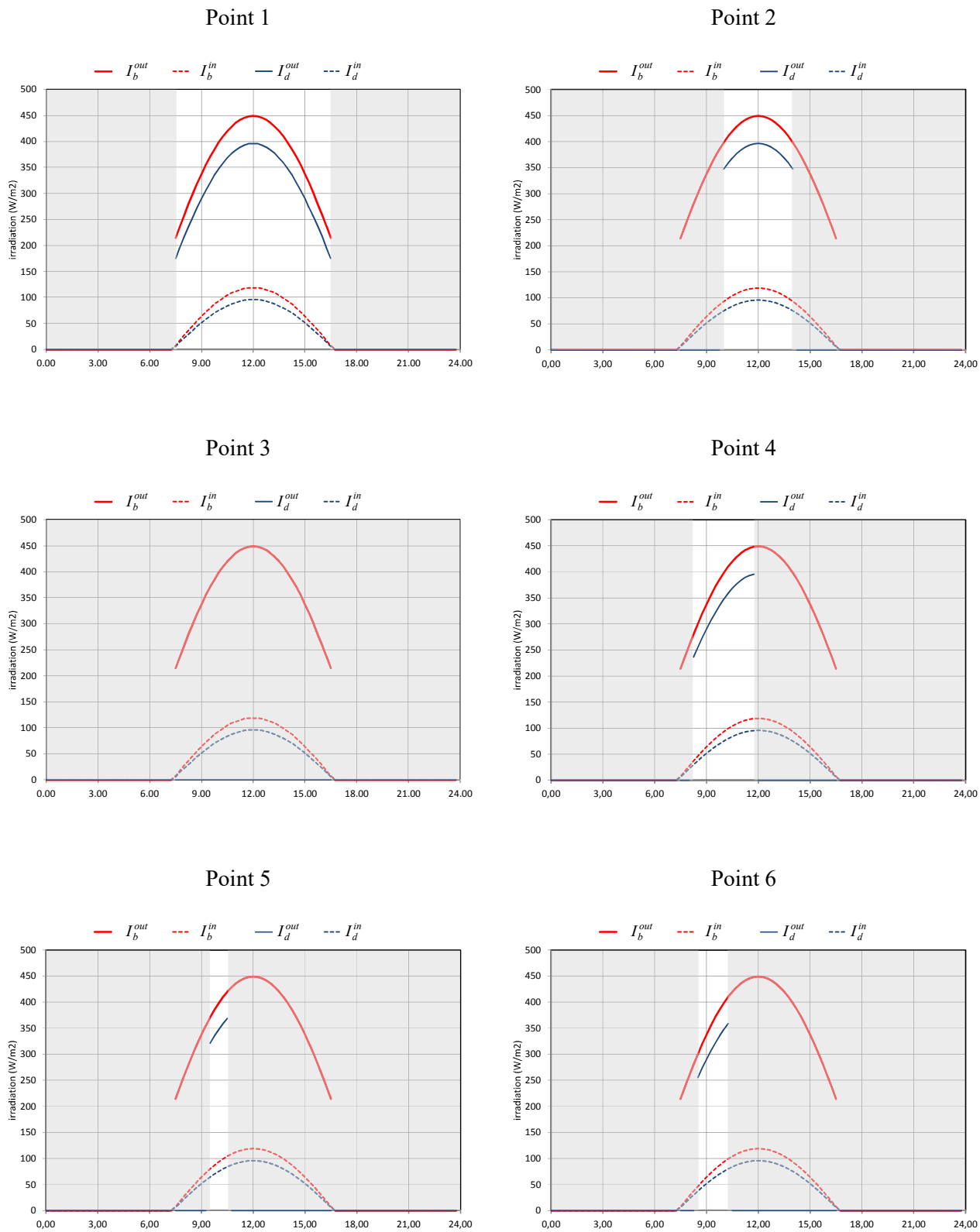

Fig. 12 – Components of solar radiation on both the outer and inner side of the glass layer and their interaction with the shadow patterns at each considered point.

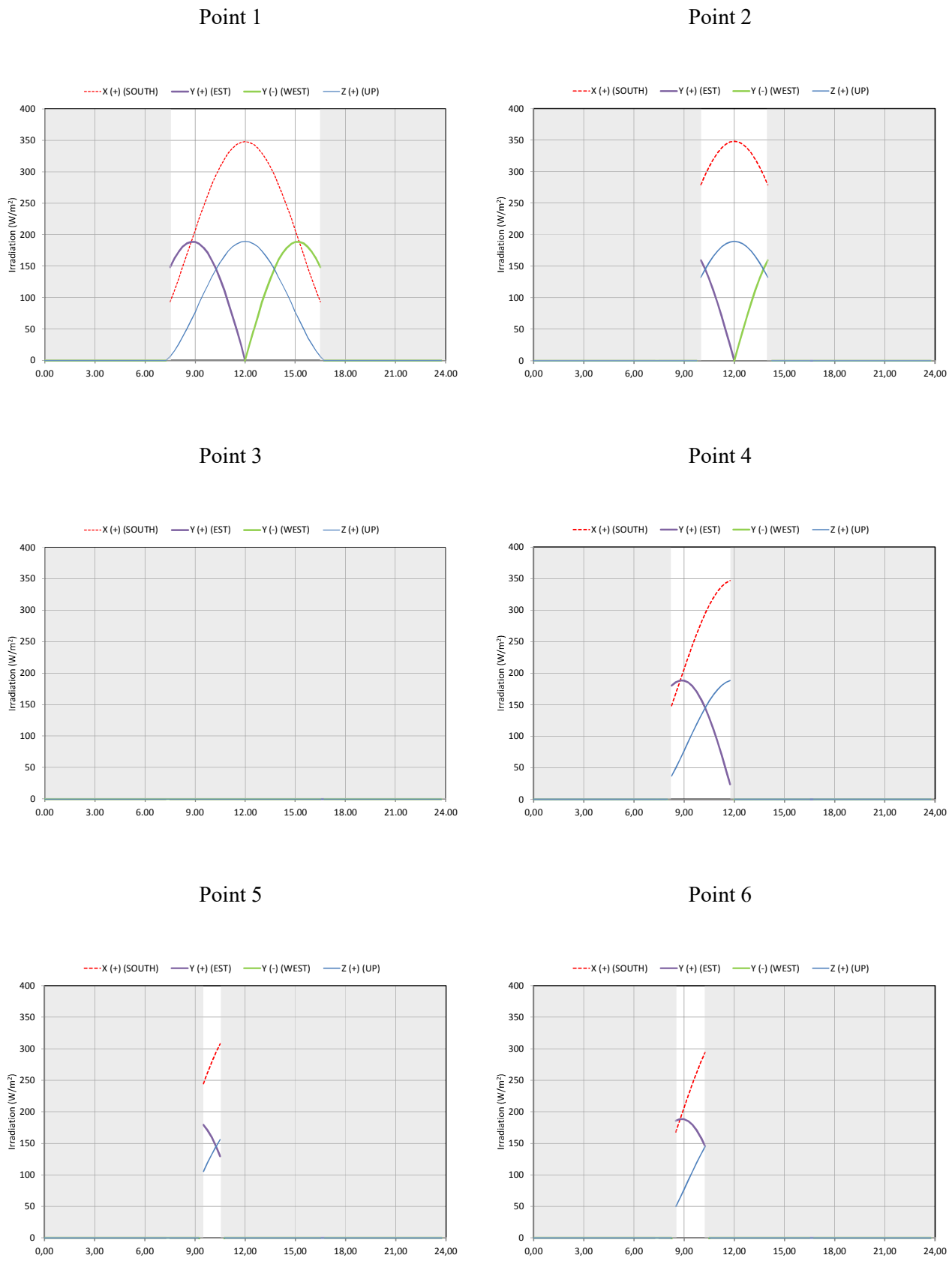

Fig. 13 – Direct radiation on the test areas and their interaction with the shadow patterns at each considered point.

As regards the contribution of the diffuse solar radiation, hypothetically coming from the window in accordance with the Lambert's Law and irradiating the test areas located at each analysed point (Fig. 14), the considerations reported in the following sections are worthy of note.

First and foremost, the diffuse component on the test areas depends on the view factor between the window and each test area; therefore:

a) for all the considered points, the X^+ test area, which faces the window, is always irradiated by diffuse radiation, whereas the North facing X^- is never affected by this phenomenon, being zero the correspondent view factors (Tab. 2);
b) at points 1, 2 and 3, the diffuse radiation, coming from the window, shines with the same intensity on the two test areas normal to the Y direction; in fact, in these cases, for symmetry reasons, the view factors between the window and the East facing test area (Y^+) are equal to the view factors between the window and the West facing test area (Y^-) (Tab. 2); on the other hand, at points 4, 5, 6 the Y^- test area is not irradiated by the diffuse radiation coming from the window, being zero the correspondent view factors;
c) for all the considered points, the Z^+ test area is always irradiated by diffuse radiation coming from the window, whereas Z^- is never affected by this phenomenon, being zero the correspondent view factor.

Point 1

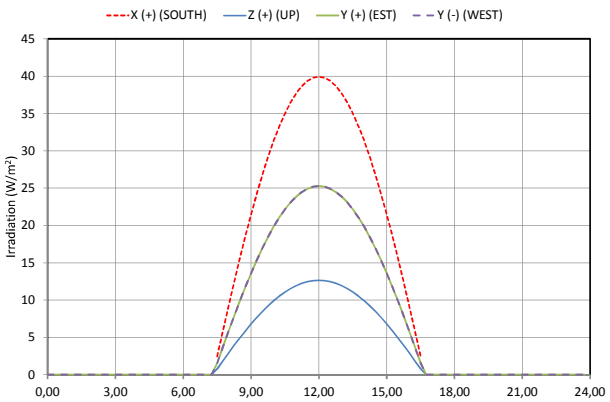

Point 2

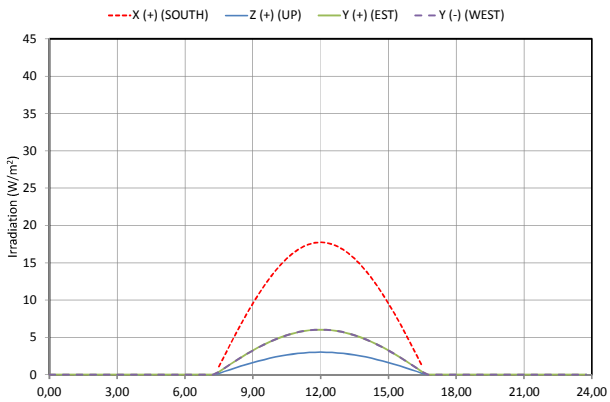

Point 3

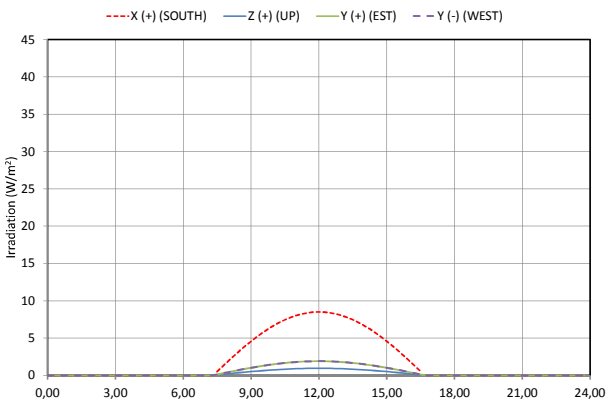

Point 4

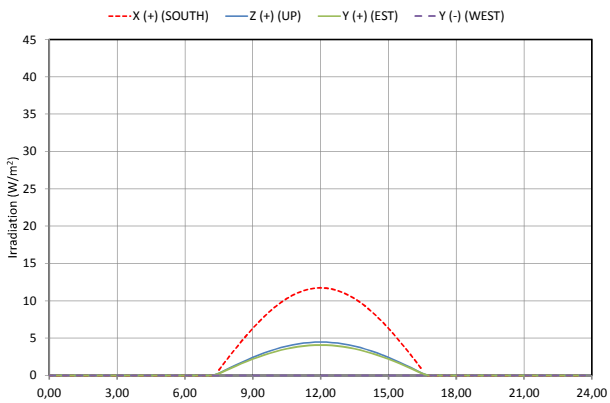

Point 5

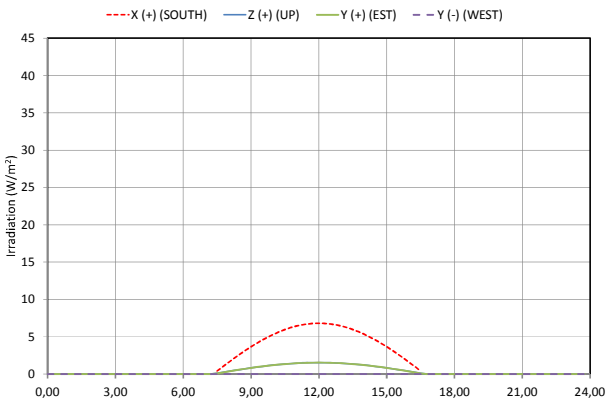

Point 6

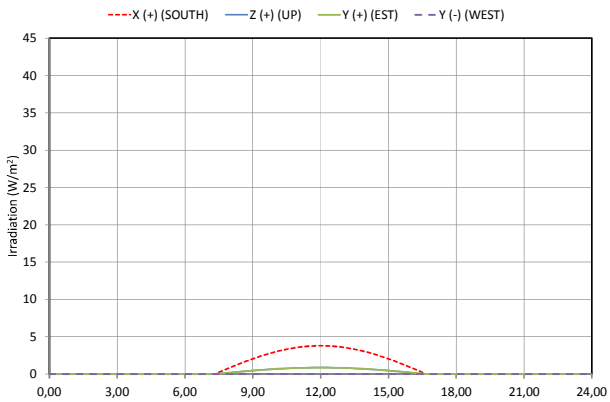

Fig. 14 – Diffuse radiation on the test areas at each considered point.

4.3 Calculation of the radiant temperature asymmetries

Both the direct and diffuse component of the solar radiation on the test areas are used in eq. (23) to assess the correspondent plane radiant temperatures, which in turn are exploited in eq. (28) to evaluate the radiant asymmetries along the three directions X, Y and Z. The time trends of the radiant asymmetries at each considered point and their connections with the shadow patterns are reported in Fig. 15.

It is worth pointing out that, at every irradiated point, the presence of the solar radiation, especially of its direct component, alters considerably the symmetry of the radiant field in the environment. In fact, the radiant asymmetries along the three directions X, Y and Z rise significantly when the considered point is irradiated by the sun, and, conversely, they decrease during the shadow periods when the direct component of solar radiation is shielded by the building envelope.

In addition, the phenomenon is also evident when the conditions of irradiated and not irradiated positions are compared. For example, the radiant asymmetries along the three directions X, Y and Z at Point 1, which is the nearest to the window and always irradiated directly by the sun, are systematically greater than the correspondent ones assessed at point 3, which is never irradiated by the direct component of the solar radiation during the studied period (Fig. 13), because of the shading effects of the building envelope.

Therefore, the major changes in the plane radiant temperature values are due to the contribution of the direct component of the solar radiation, while the effect of the diffuse one can be considered as negligible.

On balance, the analysis of these results shows that, generally, in indoor environment, the radiant asymmetry may present temporal and spatial variabilities which depend on a series of factors (view factors, solar radiations, shadow patterns, etc.) and may cause conditions of local thermal discomfort. However, it is the solar radiation, especially its direct component, which affects the radiant field the most, causing the higher values of the radiant asymmetry in the environment and restraining the zone where comfort conditions are possible.

With a view to taking this phenomenon into account, the proposed equation (23) may be conveniently utilized to both analyze the radiant field and define the suitable zones of an environment.

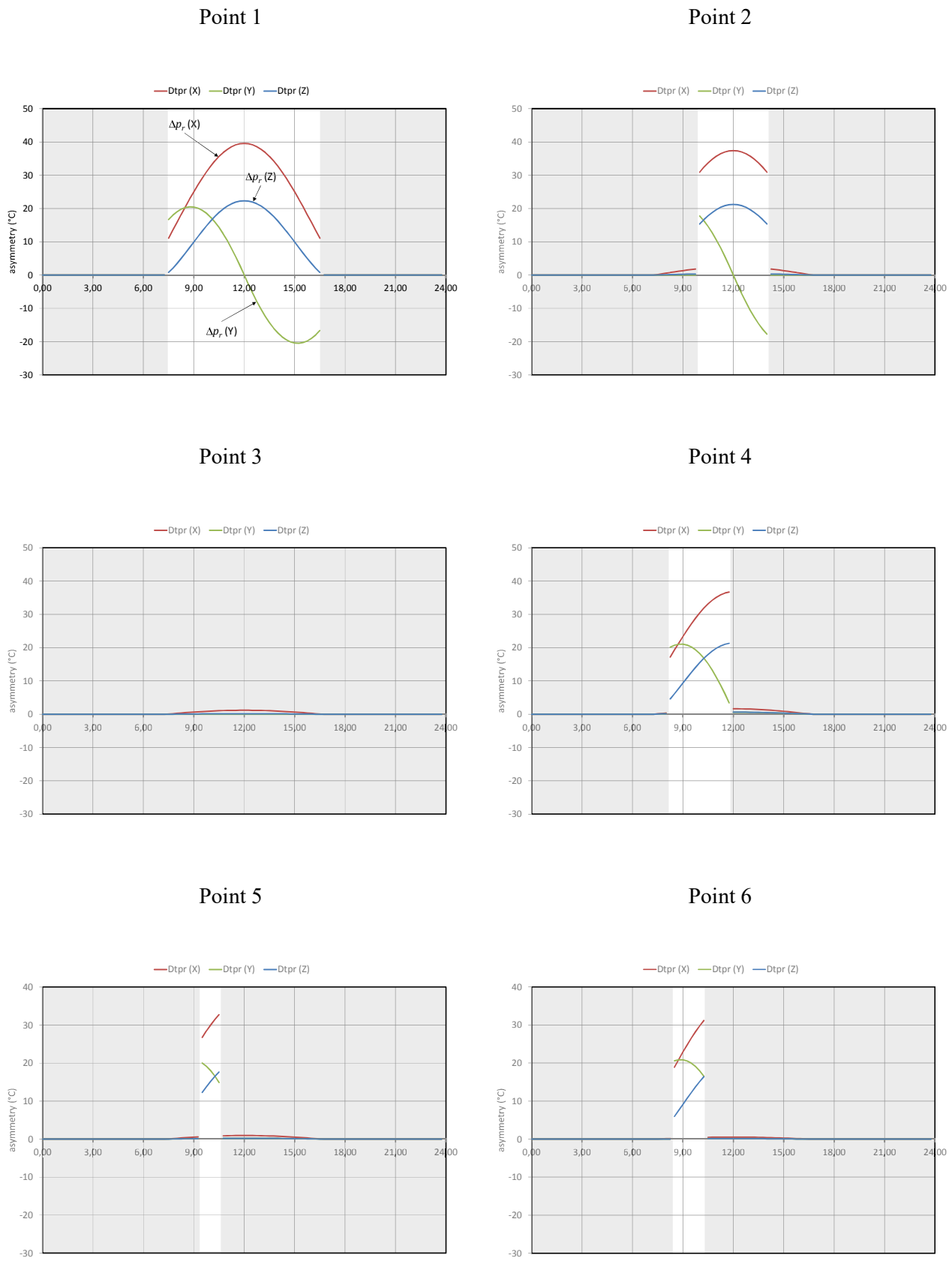

Fig. 15 – Plane radiant asymmetries at each considered point.

4.4 Indoor environmental quality: assessments regarding local thermal discomfort

In order to better understand the influence of the radiant asymmetry variability on the comfort quality of the studied environment, the last step of the analysis has concerned the assessment of the *EQI* (*Environmental Quality Index*) (Marino et al., 2012), a long time index based on the procedure reported in the EN 15217 (CEN, 2007)

It is defined as:

$$EQI = 100\bar{f}_{\mathrm{I}} + 70\bar{f}_{\mathrm{II}} + 35\bar{f}_{\mathrm{III}} \tag{32}$$

where the single factor $\bar{f}_{\mathrm{j}}$ is an indicator measuring the period of time during which the values of appropriate parameters, related to the indoor environmental conditions, persist inside specific ranges associated to levels of environmental quality. The values of $\bar{f}_{\mathrm{j}}$ form a vector named *Time Fraction Weighted Mean Vector.*

In the examined case, obviously, the parameters to be considered are the radiant asymmetries in the X, Y and Z directions, while, as regards the ranges of values defining the quality levels, the limits reported in the ISO 7730 (ISO, 2005) were used and correlated to the four environmental quality categories of the EN 15217. The result is reported in in Tab. 4.

Tab. 4 – Radiant asymmetry limits bounding the four environmental quality categories.

Parameter	**Environmental Quality Categories**			
	I	**II**	**III**	**IV**
Plane radiant asymmetry (X direction)	23	29	35	>35
Plane radiant asymmetry (Y direction)	23	29	35	>35
Plane radiant asymmetry (Z direction)	5	6	7	>7

Following the procedure reported in (Marino et al., 2012) and assuming that all the selected parameters are equally weighted, the factor $\bar{f}_{\mathrm{j}}$ is exactly the sum of the time frequencies with which the generic

environmental quality level *j* occurs at point *P*, for every considered parameter, during a reference period *T*. Therefore, it may be calculated as $\bar{f}_j = \sum_{k=1}^{3} \frac{t_{j,k}}{T}$ where $t_{j,k}$ is the period of time during which the environmental parameter *k* assumes values consistent with the level *j*, at point P, during the reference period *T*.

For the examined case, obviously, the index *k* points out to each of the three radiant asymmetries along the X, Y, and Z directions respectively, whereas T=24h; therefore, the values assumed by this parameter at each analyzed point are reported in Fig. 16.

The graph clearly shows the influence of the solar radiation: the nearer is the point to window, the longer is the period during which the point is irradiated, the higher is the frequency with which the worst quality levels (III and IV) occur.

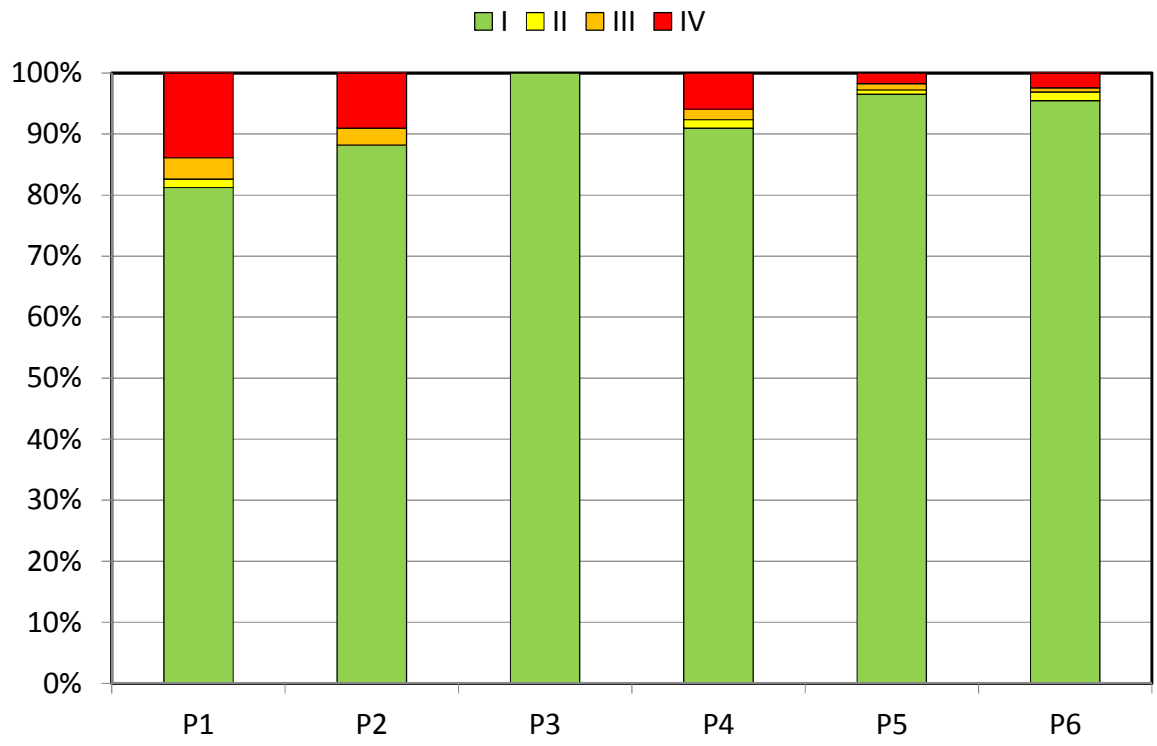

Fig. 16 – Values of the elements of the *Time Fraction Weighted Mean Vector* at each point

The calculation of the factor $\bar{f}_j$ allows an analysis of the time variability of the environmental quality at each point, but it does not allow an actual classification of the comfort conditions.

On the contrary, the EQI index is used to assign a global quality class to the environment, comprehensively taking into account all the considered characteristic parameters (namely the radiant asymmetries along the axis X, Y and Z, in the specific case) and their temporal variability. The scale of performance classes, which allows this classification task to be fulfilled, is reported in Tab. 5.

Tab. 5 – Environmental Quality classes as a function of the EQI index (Marino et al., 2012).

Values of the indexes EQI – BQI	Indoor quality class
90 – 100	A
75 – 90	B
60 – 75	C
45 – 60	D
30 – 45	E
15 – 30	F
0 – 15	G

The values of the EQIs for the analyzed case are reported in Fig. 17, where the limits of the environmental quality classes are also specified.

It is worthy of note that the lowest values of the index occur at the points which are closest to the window, where the solar radiation is present for a longer period of time; on the contrary the index shows its maximum value at the point 3, which is never irradiated by the direct component of solar radiation.

However, the EQI values remain fairly elevated, so that even in correspondence of the point P1, where the EQI value is the lowest, the environmental quality is classified as B.

This phenomenon is due to the fact that solar radiation causes environmental conditions of the worst category IV only for a limited period of time, whereas for the large part of the day category I occurs.

Nevertheless, albeit restrained in time, the environmental conditions provoked by solar direct irradiation are completely unacceptable (Fig. 15) and make the analyzed position not suitable for human activities for the high values of the radiant asymmetry.

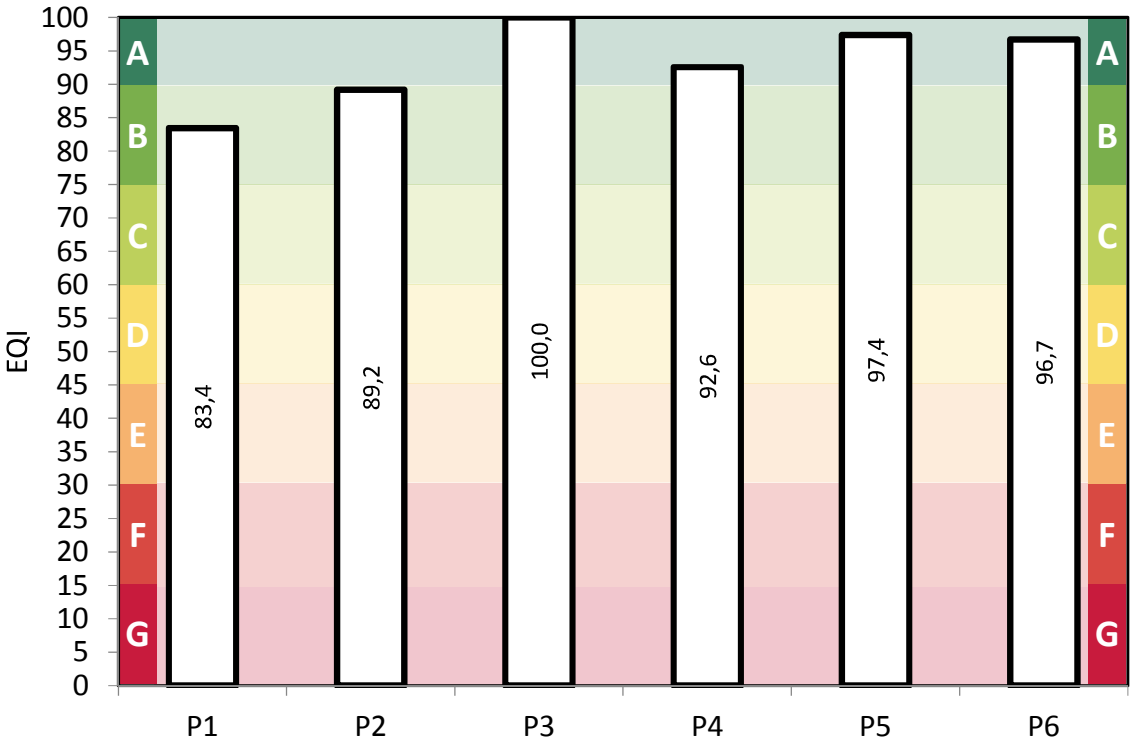

Fig. 17 – Values of the Environmental Quality Index at each studied point.

5 Conclusions

Solar radiation plays a pivotal role in building design, especially because its correct managing allows energy efficiency purpose to be fulfilled. On the other hand, solar radiation affects the radiant field inside the indoor environment and hence it has a remarkable influence on the comfort conditions, being possible cause of both local and global discomfort.

In order to properly evaluate this phenomenon, methods allowing the assessment of the human comfort conditions in presence of solar radiation are highly needed.

As far as this issue is concerned, this paper proposes a new analytical relationship for the evaluation of the asymmetry of the plane radiant temperature in a confined environment in presence of solar radiation, direct and diffuses as well.

For the proposed relationship the radiant asymmetry is a function of: (a) the temperature of the internal surfaces of the environment; (b) the intensity of the direct and diffuse component of the solar radiation; (c)

the angle factors among the opaque and glazed surfaces of the environment and the test area; (d) the incidence angle of the solar rays on the test area.

It may be conveniently utilized for studies on the radiant field, in order to identify the zones of an environment which are not suitable because of not acceptable comfort conditions. In particular, with a view to evaluating local thermal discomfort, it can allow detailed computation of the radiant asymmetry, being able to take into account the spatial and temporal variability of this parameter, which always occurs in presence of solar radiation.

Moreover, the proposed relationship may be used as part of the procedures aimed at ranking the indoor quality of edifices, in turn needed as a complement of the energy certification of buildings, as stated in Europe by the Energy Performance Building Directive (EU, 2010).

The potentiality of the proposed methodology was highlighted by means of an application to a building module, sited in a southern Italian town; for the examined case, solar radiation proved to affect the radiant asymmetry to a large extent, so that the comfort quality classification was also influenced.

In conclusion, the proposed method, taking into account the most important causes of the asymmetry of the radiant field into indoor environments, appears to be a reliable means to evaluate the presence of local discomfort. It is inferred from a theoretically basis; however, to verify its consistency from an experimental point of view, a measurement campaign is going to be designed and developed during the future stages of the current research.

Nomenclature

a	surface height [m]
A	area of the surface [m^2]
A_{AT}	area of the surface of the test area [m^2]
b	surface width [m]

C	distance between the test area and the surface [m]
C_{dn}	day–night coefficient
C_s	own-shadow coefficient
C_o	obstruction coefficient
EQI	Environmental Quality Index
F	angle factor
$\bar{f}_j$	indicator measuring the persistence in specific j^{th} class of the values of appropriate parameters
h	solar hour [h]
h_{sr}	sunrise solar hour [h]
h_{ss}	sunset solar hour [h]
I_b	intensity of the beam solar radiation [Wm^{-2}]
$I_{b\perp}$	component of the beam solar radiation perpendicular to the surface of the test area [Wm^{-2}]
I_{bh}	direct component of the solar radiation falling on a horizontal surface [Wm^{-2}]
I_b^{in}	intensity of the inner beam solar radiation [Wm^{-2}]
I_b^{out}	intensity of the external beam solar radiation [Wm^{-2}]
I_d	intensity of the diffuse solar radiation [Wm^{-2}]

I_{dh}	diffuse component of the solar radiation falling on a horizontal surface [Wm^{-2}]
I_d^{in}	intensity of the inner diffuse solar radiation [Wm^{-2}]
I_d^{out}	intensity of the outer diffuse solar radiation [Wm^{-2}]
$\dot{Q}_{AT}$	radiative net flow [W]
$\dot{Q}_{0,AT}$	emitted flux [W]
$\dot{Q}_{AT \leftrightarrow S}$	thermal flux exchanged between the test area and the environment [W]
$\dot{Q}_{b \rightarrow AT}$	direct contribution of solar radiation [W]
$\dot{Q}_{d \rightarrow AT}$	diffuse contribution of solar radiation [W]
$\dot{Q}_{env \rightarrow AT}$	long wave radiation coming from the surfaces of the environment [W]
$\dot{Q}_{sun \rightarrow AT}$	short wave solar radiation passing through the external windows [W]
$\dot{Q}_S$	thermal flow coming from the environment [W]
T	surface temperature [K]
T_{AT}	surface temperature of the test area [K]
T_{pr}	plane radiant temperature [K]
Δt_{pr}	radiant asymmetry [°C]

Greek symbols

α	solar altitude [°]
α_{AT}	absorption coefficient of the test area referred to infrared radiation
α_b	absorption coefficient of the test area referred to direct solar radiation
α_d	absorption coefficient of the test area referred to diffuse solar radiation
β	tilt angle between the surface and the horizontal [°]
θ	angle between the line normal to the surface and the solar rays [°]
ε_{AT}	emissivity of the test area
γ	solar azimuth [°]
Θ	angle between the direction of the solar rays and the normal direction to the glass [°]
ρ	albedo
σ	Stefan–Boltzmann constant ($5{,}67 \times 10^{-8}$ $Wm^{-2}K^{-4}$)
τ_b	optical transmittances of the glass for the direct component of the solar radiation
τ_d	optical transmittances of the glass for the diffuse component of the solar radiation
τ_n	optical transmittance the actual glazed surface for normal incidence
ξ	angle between the projection of the normal to the surface on a horizontal plane and the South [°]

Subscripts

AT	test area
b	beam solar radiation
d	diffuse solar radiation
env	surfaces of the environment
i	i-th isothermal surface $(i = 1.....N)$
j	j-th transparent surface $(j = 1.....M)$
n	normal
pr	plane radiant
S	environment
sun	sun

Superscripts

in	inner
out	outer

References

ASHRAE, 2010. Standard 55-2010 - Thermal environmental conditions for human occupancy. American Society of Heating, Refrigerating and Air-Conditioning Engineers, Inc. Atlanta, GA, Atlanta, GA.

ASHRAE, 1989. ASHRAE Handbook - HVAC Applications. American Society of Heating, Refrigerating and Air-Conditioning Engineers, Inc. Atlanta, GA.

Calvino, F., La Gennusa, M., Morale, M., Rizzo, G., Scaccianoce, G., 2010. Comparing different control strategies for indoor thermal comfort aimed at the evaluation of the energy cost of quality of building. Appl. Therm. Eng. 30,

2386–2395. doi:10.1016/j.applthermaleng.2010.06.008

Calvino, F., La Gennusa, M., Nucara, A., Rizzo, G., Scaccianoce, G., 2005. Evaluating human body area factors from digital images: A measurement tool for a better evaluation of the ergonomics of working places. Occup. Ergon. 5, 173–185.

CEN, 2007. EN 15217 - Energy performance of buidings - Methods for expressing energy performance and for energy certification of buildings.

EU, 2010. Directive 2010/31/EU of the European Parliament and of the Council of 19 May 2010 on the energy performance of buildings.

Fanger, P.O., 1970. Thermal comfort. Danish Technical Press, Copenhagen.

Fanger, P.O., Bànhidi, L., Olesen, B.W., Langkilde, G., 1980. Comfort Limits for heated ceilings. ASHRAE Trans. 86, 141–156.

Fanger, P.O., Ipsen, B.M., Langkilde, G., Olessen, B.W., Christensen, N.K., Tanabe, S., 1985. Comfort Limits for Asymmetric Thermal Radiation. Energy Build. 8, 225–236. doi:10.1016/0378-7788(85)90006-4

Huld, T., Müller, R., Gambardella, A., 2012. A new solar radiation database for estimating PV performance in Europe and Africa. Sol. Energy 86, 1803–1815. doi:10.1016/j.solener.2012.03.006

ISO, 2005. ISO 7730 - Ergonomics of the thermal environment - Analytical determination and interpretation of thermal comfort using calculation of the PMV and PPD indices and local thermal comfort criteria. International Standard Organization, Geneva.

ISO, 2001. EN ISO 13731 - Ergonomics of the thermal environment - Vocabulary and symbols. International Standard Organization, Geneva.

ISO, 1998. ISO 7726 - Ergonomics of the thermal environment - Instruments for measuring physical quantities. International Standard Organization, Geneva.

La Gennusa, M., Nucara, A., Pietrafesa, M., Rizzo, G., 2007. A model for managing and evaluating solar radiation for indoor thermal comfort. Sol. Energy 81, 594–606. doi:10.1016/j.solener.2006.09.005

La Gennusa, M., Nucara, A., Pietrafesa, M., Rizzo, G., Scaccianoce, G., 2008. Angle Factors and Projected Area Factors for Comfort Analysis of Subjects in Complex Confined Enclosures: Analytical Relations and Experimental Results. Indoor Built Environ. 17, 346–360. doi:10.1177/1420326X08094621

La Gennusa, M., Nucara, A., Rizzo, G., Scaccianoce, G., 2005. The calculation of the mean radiant temperature of a subject exposed to the solar radiation—a generalised algorithm. Build. Environ. 40, 367–375. doi:10.1016/j.buildenv.2004.06.019

Liu, B.Y.H., Jordan, R.C., 1960. The interrelationship and characteristic distribution of direct, diffuse and total solar radiation. Sol. Energy 4, 1–19. doi:10.1016/0038-092X(60)90062-1

Marino, C., Nucara, A., Peri, G., Pietrafesa, M., Pudano, A., Rizzo, G., 2015a. An MAS-based subjective model for indoor adaptive thermal comfort. Sci. Technol. Built Environ. 21, 114–125. doi:10.1080/10789669.2014.980683

Marino, C., Nucara, A., Pietrafesa, M., 2015b. Mapping of the indoor comfort conditions considering the effect of solar radiation. Sol. Energy 113, 63–77. doi:10.1016/j.solener.2014.12.020

Marino, C., Nucara, A., Pietrafesa, M., 2012. Proposal of comfort classification indexes suitable for both single environments and whole buildings. Build. Environ. 57, 58–67. doi:10.1016/j.buildenv.2012.04.012

Rizzo, G., Beccali, M., Nucara, A., 2004. Thermal Comfort, in: Encyclopedia of Energy. Elsevier, pp. 55–64.

Rizzo, G., Cannistraro, G., Franzitta, G., 1992. Algorithms for the calculation of the view factors between persons and rectangular surfaces in parallelepiped environments. Energy Build. 19, 51–60. doi:10.1016/0378-7788(92)90035-F

Simone, A., Della Crociata, S., Martellotta, F., 2013. The influence of clothing distribution and local discomfort on the assessment of global thermal comfort. Build. Environ. 59, 644–653. doi:10.1016/j.buildenv.2012.10.001

Tanabe, S., Narita, C., Ozeki, Y., Konishi, M., 2000. Effective radiation area of human body calculated by a numerical simulation. Energy Build. 32, 205–215. doi:10.1016/S0378-7788(00)00045-1